Late Miocene Uplift of the Tian Shan and Altai and Reorganization of Central Asia Climate

Jeremy K. Caves*, *Earth System Science, Stanford University, Stanford, California 94305, USA;* ***Bolat U. Bayshashov,*** *Institute of Zoology, Academy of Sciences, Almaty 050060, Kazakhstan;* ***Aizhan Zhamangara,*** *L.N. Gumilyov Eurasian National University, Astana 01000, Kazakhstan;* ***Andrea J. Ritch, Daniel E. Ibarra,*** *Earth System Science, Stanford University, Stanford, California 94305, USA;* ***Derek J. Sjostrom,*** *Geology Program, Rocky Mountain College, Billings, Montana 59102, USA;* ***Hari T. Mix,*** *Environmental Studies and Sciences, Santa Clara University, Santa Clara, California 95053, USA;* ***Matthew J. Winnick,*** *Geological Sciences, Stanford University, Stanford, California 94305, USA; and* ***C. Page Chamberlain,*** *Earth System Science, Stanford University, Stanford, California 94305, USA*

ABSTRACT

The timing of high surface topography and the corresponding climatic impacts of the many high ranges north of the Tibetan Plateau, such as the Altai and Tian Shan, remain poorly constrained. Most Neogene reconstructions of Central Asia climate come from interior China, where the influences of Altai and Tian Shan uplift are difficult to deconvolve from effects due to Tibetan Plateau uplift and changes in global climate. We present a new pedogenic carbonate oxygen and carbon isotope record from terrestrial Neogene sediments of the Zaysan Basin in eastern Kazakhstan, which lies upwind of the Altai and Tian Shan, in contrast to the numerous paleoclimate records from interior China. The $\delta^{18}O$ values of pedogenic carbonate exhibit a robust 4‰ decrease in the late Neogene—a trend that sharply contrasts with nearly all downwind records of $\delta^{18}O$ from Central Asia. We attribute this decrease to the establishment of the modern seasonal precipitation regime whereby Kazakhstan receives the majority of its moisture in the spring and fall, which lowers the $\delta^{18}O$ of pedogenic carbonates. The dominance of spring and fall precipitation in Kazakhstan results from the interaction of the mid-latitude jet with the high topography of the Altai and Tian Shan during its movement northward in spring and southward in fall. The late Miocene interaction of the jet with these actively uplifting northern Central Asia ranges reorganized Central Asia climate, establishing starkly different seasonal precipitation regimes, further drying interior China, and increasing the incidence of the lee cyclones that deposit dust on the Loess Plateau. We conclude that paleoclimatic changes in Central Asia in the Neogene are more tightly controlled by the interaction of the mid-latitude westerlies with the bounding ranges of northern Central Asia than by changes in the height or extent of the Tibetan Plateau.

INTRODUCTION

Research on tectonic-climatic coupling in Asia has focused primarily on the importance of the Tibetan Plateau in strengthening monsoonal circulation and in aridifying Central Asia (Zhisheng et al., 2001; Zhang et al., 2007). However, recent work places Plateau uplift in the Paleogene (Rowley and Currie, 2006), challenging the mechanisms that couple Plateau orography with increasing Central Asian aridity in the Neogene (Molnar et al., 2010; Caves et al., 2016). In contrast, many of the high ranges north of the Plateau—including the Tian Shan and Altai—appear to have uplifted more recently (Charreau et al., 2009; De Grave et al., 2007), suggesting that they may play a role in the Neogene paleoclimatic history of Central Asia (Fig. 1). Today, these ranges cast substantial rain shadows, with substantially more precipitation on their windward flanks than in the lee deserts of the Gobi and Taklamakan (Fig. 2A). Further, these ranges demarcate a stark precipitation seasonality boundary, with dominantly spring and fall precipitation to the west and primarily summertime precipitation to the east (Fig. 2B) (Baldwin and Vecchi, 2016).

Unfortunately, there is little paleoclimatic data that unequivocally indicate when the surface topography of these ranges became sufficiently prominent to impact climate in Asia. Basin analysis and sedimentological data indicate that residual topography has continuously separated many of the inward-draining basins in Central Asia since the Mesozoic (Carroll et al., 2010). Thermochronological and sedimentological studies demonstrate that reactivation of Paleozoic structures in the Tian Shan and Altai began in the late Paleogene and accelerated and/or propagated northward by the late Miocene (Charreau et al., 2009; De Grave et al., 2007). However, most paleoclimatic records in Asia come from the arid expanses of interior China, where the competing influences of uplift, Paratethys retreat, and global climate are difficult to deconvolve (Sun et al., 2013; Tang et al., 2011; Molnar et al., 2010). General circulation models (GCMs) configured with paleo-boundary conditions also produce equivocal results because their relatively low resolution hinders proper treatment of Tian Shan and Altai uplift. Therefore, most work has focused on Tibetan Plateau uplift or westward retreat of the Paratethys (Zhisheng et al., 2001; Zhang et al., 2007).

To test when the Altai and Tian Shan became sufficiently prominent to impact climate, we collected pedogenic and lacustrine carbonates for isotopic analysis from the Zaysan Basin in Kazakhstan, a long-lived basin that lies windward of the Altai

GSA Today, v. 27, no. 2, doi: 10.1130/GSATG305A.1.

*Corresponding author: jeremy.caves@gmail.com; now at Earth Surface Dynamics, ETH Zürich, 8092 Zürich, Switzerland.

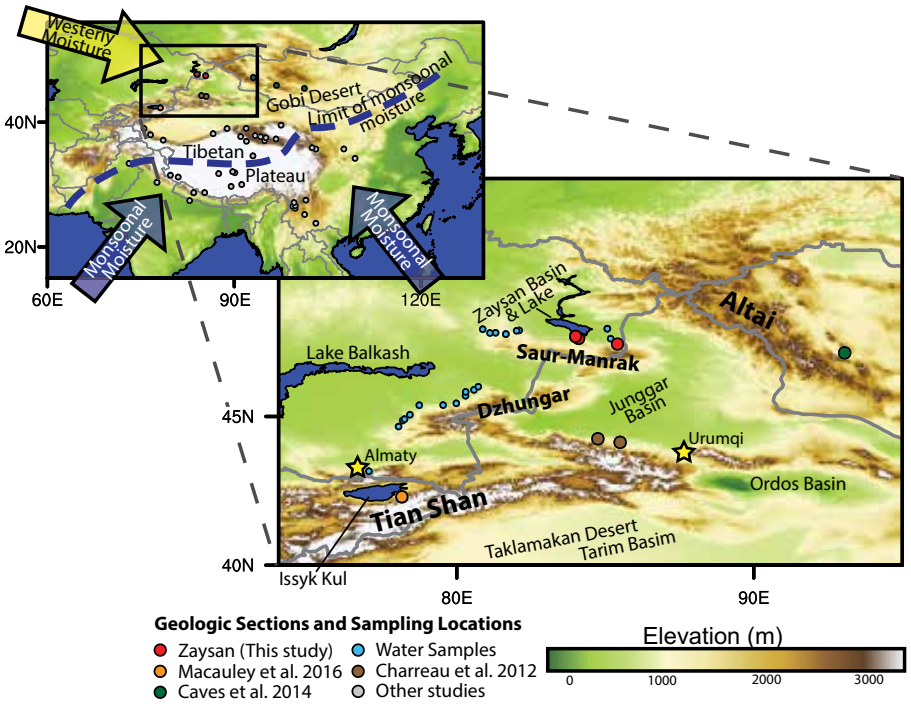

Figure 1. Location map. Inset: yellow arrow—westerly moisture; blue arrows—monsoonal moisture. Dashed blue line—approximate, modern-day inland extent of monsoonal moisture (Araguás-Araguás et al., 1998).

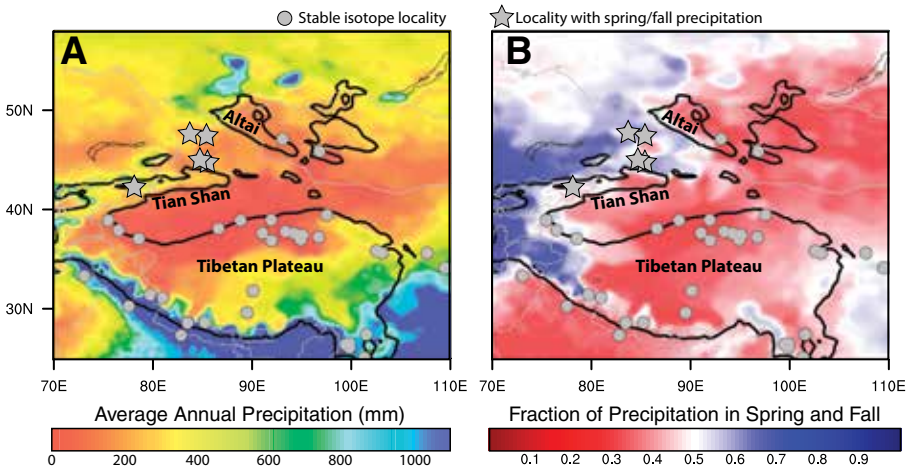

Figure 2. (A) Average annual precipitation. (B) Fraction of precipitation that falls in spring and fall versus total spring-summer-fall precipitation. Data from the Global Precipitation Climatology Center (Meyer-Christoffer et al., 2015). Gray points—Neogene sedimentary stable isotope localities; gray stars—sites impacted by spring and fall precipitation seasonality; black line—smoothed 2000 m contour. Major ranges are labeled.

and Tian Shan (Fig. 1). Oxygen isotopes ($\delta^{18}O$) are particularly sensitive to the effects of orographically forced rainout on the windward flanks of ranges (Mulch, 2016; Winnick et al., 2014), suggesting that any interaction between the Tian Shan and Altai and climate should be detectable in the Zaysan Basin. We find a 4‰ decrease in $\delta^{18}O$ in the late Neogene, which starkly contrasts with nearly all other records of sedimentary $\delta^{18}O$ from downwind localities in interior China and Mongolia that in general are constant or increasing during the Neogene (Caves et al., 2015). The timing of the $\delta^{18}O$ decrease in the Zaysan Basin is broadly synchronous with both accelerated uplift of the Tian Shan and Altai and Northern Hemisphere cooling. We attribute this decrease to a combination of sufficiently high topography and an equator-ward shift of the mid-latitude jet during cooling, which interact to create the modern spring and fall precipitation regime in Kazakhstan. The resulting climatic effects reorganized climate in Central Asia, further drying interior China and establishing the modern seasonal precipitation regime in Central Asia.

GEOLOGIC AND CLIMATIC SETTING

The Zaysan Basin (48°N; 84°E) lies in eastern Kazakhstan, bordered to the north by the Altai and to the south and east by the Saur-Manrak ranges, which separate the Zaysan Basin from the Junggar Basin (Fig. 1). These ranges are the northern end of the Dzhungar Mountains, which splay northward off the Tian Shan northeast of Almaty. As Russell and Zhai (1987, p. 158) note, "Perhaps nowhere in Asia … is there a better sequence of continental Tertiary sediments than that found in the Zaysan Basin." Though more recent work suggests substantial unconformities, sediments in the basin represent nearly every epoch since the Late Cretaceous (Lucas et al., 2009). The Paleogene and early Neogene are primarily lacustrine, which transitions to pedogenic redbeds by the late Neogene (Lucas et al., 2000).

Climatically, the Zaysan Basin is exceptionally continental, with wintertime (DJF) temperatures less than –15 °C and summertime (JJA) mean daily temperatures nearing 20 °C (Schiemann et al., 2008) (Fig. 3). Moisture is supplied entirely by the mid-latitude westerlies (Fig. 4), because high ranges to the south, including the Tian Shan, Pamir, and Hindu Kush, block subtropical air from penetrating into Kazakhstan (Schiemann et al., 2008). Notably, the Zaysan Basin lies on the border between two contrasting precipitation regimes: Kazakhstan receives the majority of its precipitation in the spring (MAM) and fall (SON), whereas interior China and Mongolia experience dominantly JJA precipitation (Baldwin and Vecchi, 2016) (Fig. 2B). This pronounced difference in precipitation seasonality is a consequence of the annual migration of the Northern Hemisphere mid-latitude jet, which swings northward in April and returns

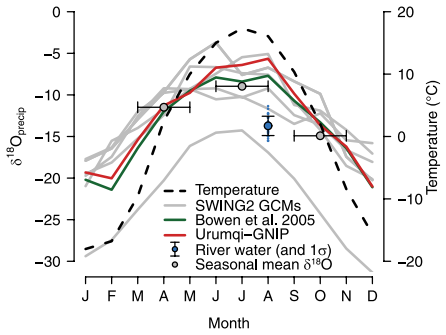

Figure 3. Average $\delta^{18}O_p$ and surface air temperature (black, dashed line) (Mitchell and Jones, 2005) in the Zaysan Basin during the year. Gray lines—SWING2 general circulation model (GCM) experiments (Risi et al., 2012); gray points—precipitation-weighted seasonal $\delta^{18}O_p$ as estimated from the SWING2 data; dark green line—Online Precipitation Isotope Calculator (Bowen et al., 2005); red line—precipitation-weighted monthly means of $\delta^{18}O_p$ from the Urumqi Global Network of Isotopes in Precipitation (GNIP) site (IAEA/WMO, 2016); blue points—measured stream water $\delta^{18}O$ in Kazakhstan.

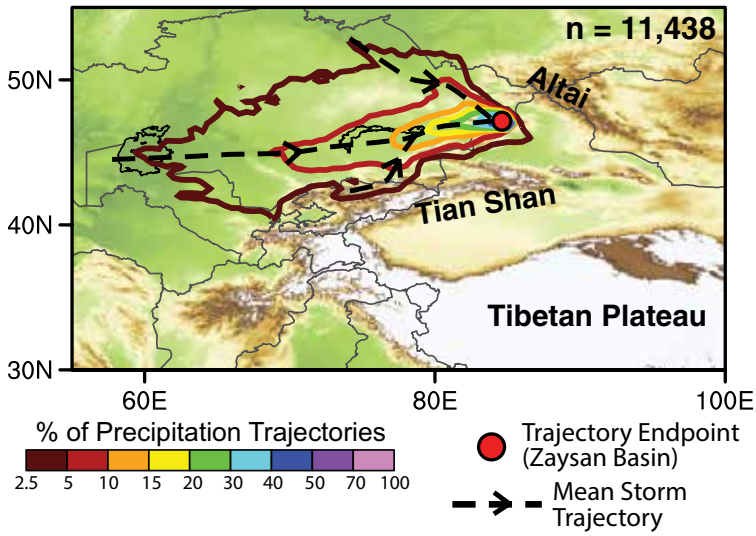

Figure 4. 2-D histogram of storm trajectories between 2005 and 2015 that produced precipitation over the Zaysan Basin, mapped using the Hybrid Single-Particle Lagrangian Integrated Trajectory Model (HYSPLIT) (Stein et al., 2015) (see the GSA Supplemental Data Repository [text footnote 1] for further details). Dashed black lines with arrows—dominant storm trajectories to the Zaysan Basin (red point). Note that all precipitation-producing storms originate to the west of the Zaysan Basin and none traverse the high topography to the south.

south in October (Schiemann et al., 2009). During this biannual migration, cyclones originating to the west interact with the Tian Shan and Altai, producing orographic precipitation (Schiemann et al., 2008, 2009; Baldwin and Vecchi, 2016).

To characterize the modern precipitation $\delta^{18}O$ ($\delta^{18}O_p$) in the Zaysan Basin, we rely upon three methods (Fig. 3). First, we interpolate estimates of $\delta^{18}O_p$ from the SWING2 (Stable Water Isotope Intercomparison Group 2) database, which uses isotopically enabled atmospheric GCMs ($n = 6$) to estimate $\delta^{18}O_p$ at ~2.5° × 2.5° resolution (Risi et al., 2012). Second, we use the Online Precipitation Isotope Calculator (Bowen et al., 2005). Third, we calculate flux-weighted $\delta^{18}O_p$ from the Urumqi, China, GNIP (Global Network of Isotopes in Precipitation) station (IAEA/WMO, 2016). All three methods produce a similar seasonal cycle, with the lowest $\delta^{18}O_p$ during DJF and the highest during JJA (Fig. 3). Average MAM and SON $\delta^{18}O_p$ is lower relative to JJA by 3.6 ± 2.3‰ and 6.8 ± 1.8‰ (1σ), respectively (gray points, Fig. 3). This seasonal cycle is characteristic of the continental air masses of Central Asia (Araguás-Araguás et al., 1998).

GEOLOGIC SAMPLING AND METHODS

We collected 77 pedogenic carbonate samples from the type-section in the Zaysan Basin along the Kalmakpay River in the southeast of the basin (47.4°N; 84.4°E). The sediments in the basin are classified into svitas (Sv.; similar to, but not strictly identical to formation) (Borisov, 1963). The upper Neogene comprises ~200 m of pedogenically altered, carbonate-rich redbeds, including the lower Kalmakpay Sv. and the upper Karabulak Sv. Kalmakpay Sv. sediments are primarily mudstones that dip ~15° NE and are separated from the yellowish sands of the underlying, carbonate-poor Sarybulak Sv. by an unconformity (Fig. 5). The overlying Karabulak Sv. is coarser, with multiple pebble conglomerates and cross-bedded sandstones that cut into pedogenic facies, and dips ~10° NE. Throughout the basin, this sequence is capped by the "Gobi Conglomerate" (Berkey and Morris, 1923), which is a Quaternary deposit (Lucas et al., 2009), from which we collected five samples of carbonate-rich cement. We also collected 54 samples from the lower Miocene, carbonate-rich, lacustrine Akzhar Sv. from the Tayzhugen and Kyzylkain River sections (Lucas et al., 2009) in the southwest of the basin. We measured carbonate $\delta^{18}O$ and $\delta^{13}C$ ($\delta^{18}O_c$ and $\delta^{13}C_c$) on a Finnigan MAT Delta+ XL mass spectrometer at the Stable Isotope Biogeochemistry Laboratory (Stanford University, California, USA; see the GSA Supplemental Data Repository[1] for full methods).

The ages of these sediments are constrained by biostratigraphy and magnetostratigraphy. The Akzhar Sv. is assigned to the Shanwangian Asian Land Mammal Age (ALMA) (16.9–13.7 Ma), and the overlying Sarybulak Sv. is assigned to the Tunggurian ALMA (13.7–11.1 Ma) (Kowalski and Shevyreva, 1997). The Karabulak Sv. contains abundant "Hipparion" fauna, which is correlated with the latest Turolian (8.7–5.3 Ma; latest Baodean ALMA) (Sotnikova et al., 1997; Vangengeim et al., 1993; Lucas et al., 2009). The intervening Kalmakpay Sv. is not as clearly constrained by mammal fossils, yet is a separate unit from the overlying Karabulak Sv. Following Vangengeim et al. (1993) and Lucas et al. (2009), we therefore place the lower boundary in the

[1] GSA Supplemental Data Repository Item 2017024, containing methods, additional climatology, sedimentary, and diagenetic background and discussion, figures and tables, is online at http://www.geosociety.org/datarepository/2017/. If you have questions, please email gsatoday@geosociety.org.

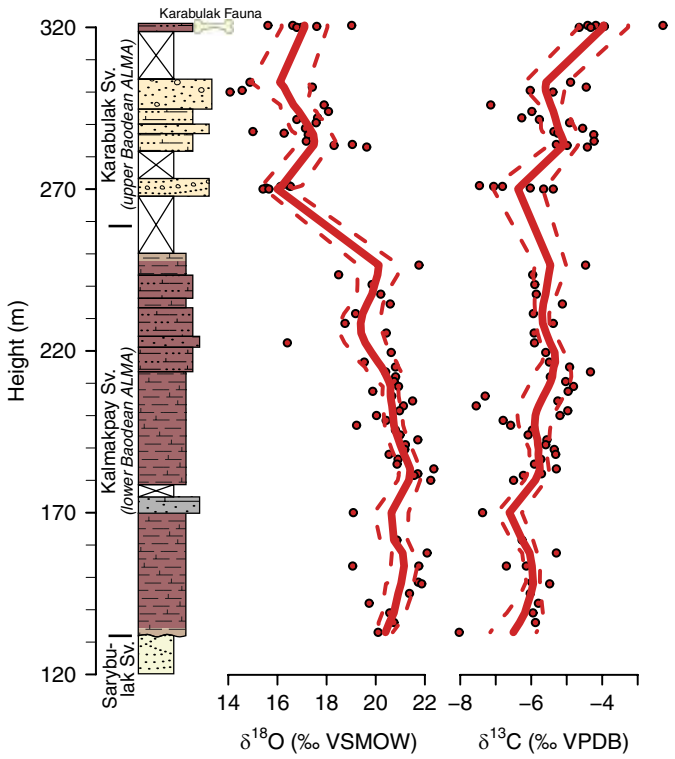

Figure 5. $\delta^{18}O$ and $\delta^{13}C$ of pedogenic carbonates from the Kalmakpay River section against stratigraphic height. Solid and dashed red lines are a kernel-smooth of the data using an Epanechnikov kernel (mean and 1σ) with a 6 m bandwidth. Data from the overlying Gobi Conglomerate and underlying Akzhar Sv. are not shown (see Fig. 6). Sv.—svita; VSMOW—Vienna Standard Mean Ocean Water; VPDB—Vienna Pee Dee belemnite.

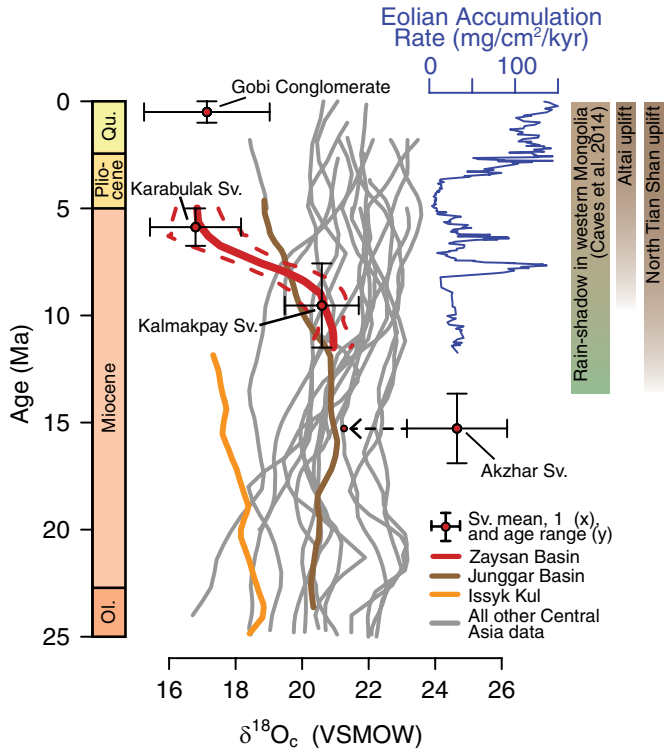

Figure 6. $\delta^{18}O$ data from Zaysan plotted against age. Red points are mean svita $\delta^{18}O$ with 1σ uncertainty (*x*) and possible age range (*y*). Data from the Karabulak and Kalmakpay Sv. are smoothed using 1 Ma bandwidth Epanechnikov kernel (solid red line) with 1σ uncertainty (dashed red lines). Also plotted are published data from Central Asia (gray lines), Issyk Kul (orange line; Macaulay et al., 2016), and the Junggar Basin (brown line; Charreau et al., 2012). All are smoothed using an Epanechnikov kernel with 1 Ma bandwidth, after Caves et al. (2015). For the Akzhar Sv., we also plot the minimum $\delta^{18}O$ value (small red point) due to evaporative enrichment in this svita. Eolian accumulation rate, as recorded by North Pacific deep-sea records (Rea et al., 1998), is a proxy for loess production. Note the prominent peak coincident with decreasing $\delta^{18}O_c$. Regional climatic and tectonic events are listed to the right. Shading indicates uncertainty in the timing of uplift and rain shadow development. Ol.—Oligocene; Qu.—Quaternary; Sv.—svita; VSMOW—Vienna Standard Mean Ocean Water.

late Sarmatian (12.7–11.6 Ma) and the upper boundary in the lower Baodean ALMA. To account for the uncertainty in using this chronologic scheme, we present the data against both height (Fig. 5) and plotted against age (Fig. 6), where we bin the data by svita and assume that the sediments in each svita could have been deposited at any interval during the ALMA.

We also collected 29 stream and well-water samples to characterize the $\delta^{18}O$ of modern waters in Kazakhstan. Stream waters integrate $\delta^{18}O$ across storm and snowmelt events and are used to characterize modern water $\delta^{18}O$ where $\delta^{18}O_p$ data are sparse (Hoke et al., 2014). We measured water $\delta^{18}O$ on a Los Gatos Research TWIA-45EP liquid isotope water analyzer at Santa Clara University, California, USA.

RESULTS

The mean Kalmakpay Sv. $\delta^{18}O_c$ (20.6‰) is significantly 4‰ higher than the mean $\delta^{18}O_c$ of the Karabulak Sv. (16.8‰) (Fig. 5). Similarly, there is a slight, but significant, increase in the mean $\delta^{13}C_c$ from the Kalmakpay Sv. (–5.8‰) to the Karabulak Sv. (–5.2‰). Using an estimate of the mean value (solid, red line in Fig. 5), $\delta^{13}C_c$ increases 2.5‰ from the base of the section to the top. The overlying Gobi Conglomerate samples have equivalent $\delta^{18}O_c$ as the underlying Karabulak samples, but higher $\delta^{13}C_c$.

Samples from the Akzhar Sv. show the greatest spread in $\delta^{13}C_c$ and $\delta^{18}O_c$ and the mean $\delta^{18}O_c$ (24.7‰) is significantly higher than the overlying svitas (see GSA supplemental data Table S1). Given the correlation between $\delta^{18}O_c$ and carbonate content (supplemental data Fig. S2), we treat these $\delta^{18}O_c$ data as evaporatively enriched. Following other studies in Central Asia (Rowley and Currie, 2006), we therefore consider the minimum $\delta^{18}O_c$ value as closest to the $\delta^{18}O_p$ value.

Stream/well water $\delta^{18}O$ ranges from –15.5‰ to –11.3‰ (mean = –13.7‰) (supplemental data Table S2). This mean value is less than the estimated value of MAM $\delta^{18}O_p$ (–12.3‰) and substantially less than the estimated value of JJA $\delta^{18}O_p$ (–8.6‰). These samples were collected from streams that drain the 2500+ m Manrak-Saur-Dzhungar ranges and therefore likely integrate $\delta^{18}O$ in catchments potentially still influenced by snowmelt and with large variations in elevation (Hoke et al., 2014).

DISCUSSION

The most prominent trend in our record is the 4‰ decrease in $\delta^{18}O_c$ that occurs in the late Neogene. This trend is opposite to nearly all other $\delta^{18}O_c$ records in Central Asia that lie downwind of the Zaysan Basin and either increase or remain approximately constant over the Neogene (Fig. 6) (Caves et al., 2015). Notably, the only other records that decrease during the Neogene are those that also lie on the windward flank of the Tian Shan (Issyk Kul) and/or within the modern-day spring and fall precipitation regime (Junggar Basin) (gray stars; Fig. 2B).

What mechanisms might explain a simultaneous decrease in $\delta^{18}O$ on the windward flanks of the Tian Shan and Altai, while permitting constant or increasing $\delta^{18}O$ in their lee?

One potential mechanism is that increased orographic precipitation due to uplift might shift windward $\delta^{18}O$ to lower values, particularly as high-elevation precipitation is increasingly captured (Mulch, 2016). This hypothesis has been used to explain the decrease in $\delta^{18}O$ at both Issyk Kul and the Junggar Basin (Charreau et al., 2012; Macaulay et al., 2016). However, increased orographic precipitation appears unlikely to explain the full decrease in the Zaysan Basin. The long-term increase in $\delta^{13}C$ in the Zaysan Basin—at a location well north of where abundant C_4 vegetation is typically found (supplemental data Fig. S3)—indicates that soil respiration rates dropped, suggesting a decline in productivity and, hence, precipitation (Breecker et al., 2009; Caves et al., 2016). Further, increased orographic precipitation should also result in coupled $\delta^{18}O$ decreases in the lee of these ranges, which is not observed, though $\delta^{18}O_c$ in lee basins is complicated by evaporative effects (Mulch, 2016). An additional mechanism could be an increase in the formation temperature of pedogenic carbonate, given that the fractionation of ^{18}O between water and calcite decreases as temperature increases (~−0.2‰/°C) (Kim and O'Neil, 1997). However, an increase in temperature is unlikely because global climate cooled in the late Neogene following the Miocene Climatic Optimum (Zachos et al., 2001). Further, if changes in global temperature were the dominant factor driving changes in $\delta^{18}O_c$, one would expect similar decreases across much of northern Central Asia, which are not observed (Caves et al., 2015).

In contrast to the above two mechanisms, shifting precipitation seasonality in Kazakhstan might have a substantial effect on $\delta^{18}O_c$ given the large seasonal $\delta^{18}O_p$ changes observed in Central Asia (Fig. 3) (Araguás-Araguás et al., 1998). Pedogenic carbonates are seasonally biased recorders of $\delta^{18}O_p$, typically recording wet-season $\delta^{18}O_p$ (Breecker et al., 2009). Thus, a shift toward dominantly spring and fall precipitation might change the timing of pedogenic carbonate formation and decrease $\delta^{18}O_c$, without necessarily increasing total precipitation. Such a shift may have also lowered the temperature of carbonate formation, raising $\delta^{18}O_c$, and partially offsetting the true change in precipitation-weighted $\delta^{18}O_p$; this implies that the change in precipitation seasonality may have been substantial. Importantly, this change in precipitation seasonality would decouple windward $\delta^{18}O_c$ records (Zaysan, Issyk Kul, and Junggar) from leeward $\delta^{18}O_c$ records in interior China and Mongolia, which receive dominantly JJA precipitation.

IMPLICATIONS

The modern spring and fall precipitation regime in Kazakhstan is a result of the interaction between cyclones routed along the mid-latitude westerly jet as it migrates seasonally north and south and the high topography of the Tian Shan and Altai (Schiemann et al., 2009). Thus, a change in precipitation seasonality would imply either a shift of the mid-latitude jet, the development of high topography, or both. The mean position of the jet is thought to have been farther northward during the late Miocene given warmer Arctic temperatures (Micheels et al., 2011), suggesting that cooling into the late Miocene may have contributed to a southward shift of the jet.

Further, northward growth of high topography in Asia would result in increased interaction between cyclones routed along the jet and this topography, resulting in orographic precipitation during the spring and fall (Baldwin and Vecchi, 2016). There is substantial evidence that deformation from the collision of India-Asia has propagated northward during the Cenozoic, resulting in—most recently in the latest Miocene—uplift of the Altai range (De Grave et al., 2007). The Altai rain shadow likely formed by the latest Miocene, as indicated by a substantial increase in pedogenic carbonate $\delta^{13}C$ in the lee of the Altai (Caves et al., 2014) (Fig. 6). In the northern Tian Shan, Charreau et al. (2009) found increased sedimentation rates in the Junggar Basin at ca. 11 Ma, which they proposed resulted from an acceleration of uplift. Though the individual uplift histories of the local Saur-Manrak ranges are unknown, but are likely linked to uplift in the Altai or northern Tian Shan (Campbell et al., 2013), we propose that the timing of this accelerated uplift is broadly synchronous with our observed decrease in $\delta^{18}O_c$. Northward-propagating deformation might also explain why oxygen isotopic records from Issyk Kul, which lies 5° south, decline starting in the early Miocene, reflecting earlier growth of high topography to the south (Macaulay et al., 2016).

Our new oxygen isotope record from the windward side of the Tian Shan and Altai ranges indicates that these ranges were sufficiently elevated by the late Miocene to impact climate in Central Asia. Most notably, this interaction resulted in a substantial reorganization of Central Asia climate, creating a stark precipitation seasonality boundary between eastern and western Central Asia. Such high topography would have further blocked moisture from reaching downwind Central Asia, contributing to the increasingly arid conditions and formation of the Taklamakan and Gobi deserts in the late Miocene (Caves et al., 2016; Sun et al., 2009). The Altai are the largest source of lee cyclones in Asia (Chen et al., 1991), and the combined interaction of high topography with the jet's oscillations as it moves northward in the spring (Schiemann et al., 2009) creates the dust storms that blanket the Loess Plateau (Shao and Dong, 2006; Roe, 2009). Thus, acceleration of loess deposition in the late Miocene (Zhang et al., 2014; Rea et al., 1998) may be a consequence of increasing cyclogenesis as a result of upwind topographic growth (Caves et al., 2014; Shi et al., 2015) (Fig. 6). The subsequent Pliocene decline in eolian accumulation rates may reflect a northward shifted jet during the mid-Pliocene Warm Period, which precluded interaction with the Altai until Quaternary cooling shifted the jet southward again.

We conclude that uplift of the Tian Shan and Altai reorganized late Neogene climate in Central Asia, establishing a prominent seasonal precipitation boundary as a result of increasing interactions between the mid-latitude jet and high topography. Thus, paleoclimatic changes in Central Asia in the late Neogene may not be due solely to changes in the extent or height of the Tibetan Plateau. In contrast, the timing of uplift and consequent climatic impacts of Asia's northern bounding ranges are critical to unraveling the paleoenvironmental history of Central Asia. Ultimately, future work to test this interpretation must include westward/upwind records of $\delta^{18}O$ combined with GCM studies that resolve the impact of Tian Shan and Altai uplift on Asian climate.

ACKNOWLEDGMENTS

We thank our field expedition members, including B. Dautaliev, G. Nazyanbeteva, S. Samzatbaeva, J. Buztsev, and S. Bayshashov, and N. Ballantine, D. Moragne, and P. Blisniuk for assistance with lab work. We also thank two anonymous reviewers and editor G. Dickens for comments that improved the manuscript. A GSA Student Research grant (Caves), three Stanford University McGee grants (Caves, Ritch, and Ibarra), and NSF grants EAR-1009721 and EAR-1423967 (Chamberlain) funded this work. Caves is also funded by an NSF Graduate Research Fellowship (DGE-1147470) and a Stanford Graduate Fellowship.

REFERENCES CITED

Araguás-Araguás, L., Froehlich, K., and Rozanski, K., 1998, Stable isotope composition of precipitation over southeast Asia: Journal of Geophysical Research, v. 103, D22, p. 28,721–28,742, doi: 10.1029/98JD02582.

Baldwin, J., and Vecchi, G., 2016, Influence of the Tianshan Mountains on arid extratropical Asia: Journal of Climate, v. 29, p. 5741–5762, doi: 10.1175/JCLI-D-15-0490.1.

Berkey, C.P., and Morris, F.K., 1923, Geology of Mongolia—A Reconnaissance Report Based on the Investigations of the Years 1922–1923: New York, American Museum of Natural History, 475 p.

Borisov, B.A., 1963, [The stratigraphy of the Upper Cretaceous and of the Paleogene-Neogene of the Zaysan Depression] Stratigrafiya verkhnego mela i paleogen-neogena Zaysanskoy vvpadiny. Materiali po geologii i poleznym iskopayemym Altaya i Kazakhstana: Trudy VSEGEI i Gos: Geol. Komenta, v. 94, p. 11–75.

Bowen, G.J., Wassenaar, L.I., and Hobson, K.A., 2005, Global application of stable hydrogen and oxygen isotopes to wildlife forensics: Oecologia, v. 143, no. 3, p. 337–348, doi: 10.1007/s00442-004-1813-y.

Breecker, D.O., Sharp, Z.D., and McFadden, L.D., 2009, Seasonal bias in the formation and stable isotopic composition of pedogenic carbonate in modern soils from central New Mexico, USA: GSA Bulletin, v. 121, no. 3–4, p. 630–640, doi: 10.1130/B26413.1.

Campbell, G.E., Walker, R.T., Abdrakhmatov, K., Schwenninger, J., Jackson, J., Elliott, J.R., and Copley, A., 2013, The Dzhungarian fault: Late Quaternary tectonics and slip rate of a major right-lateral strike-slip fault in the northern Tien Shan region: Journal of Geophysical Research, Solid Earth, v. 118, no. 10, p. 5681–5698, doi: 10.1002/jgrb.50367.

Carroll, A.R., Graham, S.A., and Smith, M.E., 2010, Walled sedimentary basins of China: Basin Research, v. 22, no. 1, p. 17–32, doi: 10.1111/j.1365-2117.2009.00458.x.

Caves, J.K., Sjostrom, D.J., Mix, H.T., Winnick, M.J., and Chamberlain, C.P., 2014, Aridification of Central Asia and uplift of the Altai and Hangay Mountains, Mongolia: Stable isotope evidence: American Journal of Science, v. 314, no. 8, p. 1171–1201, doi: 10.2475/08.2014.01.

Caves, J.K., Winnick, M.J., Graham, S.A., Sjostrom, D.J., Mulch, A., and Chamberlain, C.P., 2015, Role of the westerlies in Central Asia climate over the Cenozoic: Earth and Planetary Science Letters, v. 428, p. 33–43, doi: 10.1016/j.epsl.2015.07.023.

Caves, J.K., Moragne, D.Y., Ibarra, D.E., Bayshashov, B.U., Gao, Y., Jones, M.M., Zhamangara, A., Arzhannikova, A.V., Arzhannikov, S.G., and Chamberlain, C.P., 2016, The Neogene de-greening of Central Asia: Geology, v. 44, no. 11, p. 887–890, doi: 10.1130/G38267.1.

Charreau, J., Chen, Y., Gilder, S., Barrier, L., Dominguez, S., Augier, R., Sen, S., Avouac, J.-P., Gallaud, A., Graveleau, F., and Wang, Q., 2009, Neogene uplift of the Tian Shan Mountains observed in the magnetic record of the Jingou River section (northwest China): Tectonics, v. 28, no. 2, TC2008, doi: 10.1029/2007TC002137.

Charreau, J., Kent-Corson, M.L., Barrier, L., Augier, R., Ritts, B.D., Chen, Y., France-Lannord, C., and Guilmette, C., 2012, A high-resolution stable isotopic record from the Junggar Basin (NW China): Implications for the paleo-topographic evolution of the Tianshan Mountains: Earth and Planetary Science Letters, v. 341–344, p. 158–169, doi: 10.1016/j.epsl.2012.05.033.

Chen, S., Kuo, Y., Zhang, P., and Bai, Q., 1991, Synoptic climatology of cyclogenesis over East Asia, 1958–1987: Monthly Weather Review, v. 119, p. 1407–1418, doi: 10.1175/1520-0493(1991)119<1407:SCOCOE>2.0.CO;2.

De Grave, J., Buslov, M.M., and van den Haute, P., 2007, Distant effects of India–Eurasia convergence and Mesozoic intracontinental deformation in Central Asia: Constraints from apatite fission-track thermochronology: Journal of Asian Earth Sciences, v. 29, no. 2–3, p. 188–204, doi: 10.1016/j.jseaes.2006.03.001.

Hoke, G.D., Liu-Zeng, J., Hren, M.T., Wissink, G.K., and Garzione, C.N., 2014, Stable isotopes reveal high southeast Tibetan Plateau margin since the Paleogene: Earth and Planetary Science Letters, v. 394, p. 270–278, doi: 10.1016/j.epsl.2014.03.007.

IAEA/WMO, 2016, Global Network of Isotopes in Precipitation: The GNIP Database: http://www.iaea.org/water.

Kim, S., and O'Neil, J., 1997, Equilibrium and nonequilibrium oxygen isotope effects in synthetic carbonates: Geochimica et Cosmochimica Acta, v. 61, no. 16, p. 3461–3475, doi: 10.1016/S0016-7037(97)00169-5.

Kowalski, K., and Shevyreva, N.S., 1997, *Gliridae* (Mammalia: Rodentia) from the Miocene of the Zaisan Depression (Eastern Kazakhstan): Acta Zoologica Cracoviensia, v. 40, no. 2, p. 199–208.

Lucas, S.G., Aubekerov, B.Z., Dzhamangaraeva, A., Bayshashov, B.U., and Tyutkova, L.A., 2000, Cenozoic lacustrine deposits of the Ili Basin, southeastern Kazakhstan, *in* Gierlowski-Kordesch, E., and Kelts, K., eds., Lake Basins through Space and Time: AAPG Studies in Geology, v. 46, p. 59–64.

Lucas, S.G., Emry, R.J., Bayshashov, B., and Tyutkova, L., 2009, Cenozoic mammalian biostratigraphy and biochronology in the Zaysan Basin, Kazakstan: Museum of Northern Arizona Bulletin, v. 65, p. 621–634.

Macaulay, E.A., Sobel, E.R., Mikolaichuk, A., Wack, M., Gilder, S.A., Mulch, A., Fortuna, A.B., Hynek, S., and Apayarov, F., 2016, The sedimentary record of the Issyk Kul basin, Kyrgyzstan: Climatic and tectonic inferences: Basin Research, v. 28, p. 57–80, doi: 10.1111/bre.12098.

Meyer-Christoffer, A., Becker, A., Finger, P., Rudolf, B., Schneider, U., and Ziese, M., 2015, GPCC Climatology Version 2015 at 0.25°: Monthly land-surface precipitation climatology for every month and the total year from rain-gauges built on GTS-based and historic data: Global Precipitation Climatology Centre (GPCC) at Deutscher Wetterdienst, http://gpcc.dwd.de/, doi: 10.5676/DWD_GPCC/CLIM_M_V2015_025.

Micheels, A., Bruch, A.A., Eronen, J., Fortelius, M., Harzhauser, M., Utescher, T., and Mosbrugger, V., 2011, Analysis of heat transport mechanisms from a Late Miocene model experiment with a fully coupled atmosphere–ocean general circulation model: Palaeogeography, Palaeoclimatology, Palaeoecology, v. 304, no. 3–4, p. 337–350, doi: 10.1016/j.palaeo.2010.09.021.

Mitchell, T.D., and Jones, P.D., 2005, An improved method of constructing a database of monthly climate observations and associated high-resolution grids: International Journal of Climatology, v. 25, no. 6, p. 693–712, doi: 10.1002/joc.1181.

Molnar, P., Boos, W.R., and Battisti, D.S., 2010, Orographic controls on climate and paleoclimate of Asia: Thermal and mechanical roles for the Tibetan Plateau: Annual Review of Earth and Planetary Sciences, v. 38, no. 1, p. 77–102, doi: 10.1146/annurev-earth-040809-152456.

Mulch, A., 2016, Stable isotope paleoaltimetry and the evolution of landscapes and life: Earth and Planetary Science Letters, v. 433, p. 180–191, doi: 10.1016/j.epsl.2015.10.034.

Rea, D.K., Snoeckx, H., and Joseph, L.H., 1998, Late Cenozoic eolian deposition in the North Pacific: Asian drying, Tibetan uplift, and cooling of the northern hemisphere: Paleoceanography, v. 13, no. 3, p. 215–224, doi: 10.1029/98PA00123.

Risi, C., and 29 others, 2012, Process-evaluation of tropospheric humidity simulated by general circulation models using water vapor isotopologues: 1. Comparison between models and observations: Journal of Geophysical Research, D, Atmospheres, v. 117, no. 5, D05303, doi: 10.1029/2011JD016621.

Roe, G., 2009, On the interpretation of Chinese loess as a paleoclimate indicator: Quaternary Research, v. 71, no. 2, p. 150–161, doi: 10.1016/j.yqres.2008.09.004.

Rowley, D.B., and Currie, B.S., 2006, Palaeo-altimetry of the late Eocene to Miocene Lunpola basin, central Tibet: Nature, v. 439, p. 677–681, doi: 10.1038/nature04506.

Russell, D., and Zhai, R., 1987, The Paleogene of Asia: Mammals and Stratigraphy: Paris Museum National d'Histoire Naturelle, v. 2, 488 p.

Schiemann, R., Lüthi, D., Vidale, P.L., and Schär, C., 2008, The precipitation climate of Central Asia—Intercomparison of observational and numerical data sources in a remote semiarid region: International Journal of Climatology, v. 28, p. 295–314, doi: 10.1002/joc.1532.

Schiemann, R., Lüthi, D., and Schär, C., 2009, Seasonality and interannual variability of the westerly jet in the Tibetan Plateau region: Journal of Climate, v. 22, no. 11, p. 2940–2957, doi: 10.1175/2008JCLI2625.1.

Shao, Y., and Dong, C.H., 2006, A review on East Asian dust storm climate, modelling and monitoring: Global and Planetary Change, v. 52, p. 1–22, doi: 10.1016/j.gloplacha.2006.02.011.

Shi, Z., Liu, X., Liu, Y., Sha, Y., and Xu, T., 2015, Impact of Mongolian Plateau versus Tibetan Plateau on the westerly jet over North Pacific Ocean: Climate Dynamics, v. 44, p. 3067–3076, doi: 10.1007/s00382-014-2217-2.

Sotnikova, M., Dodonov, A., and Pen'kov, A., 1997, Upper Cenozoic bio-magnetic stratigraphy of Central Asian mammalian localities: Palaeogeography, Palaeoclimatology, Palaeoecology, v. 133, p. 243–258, doi: 10.1016/S0031-0182(97)00078-3.

Stein, A.F., Draxler, R.R., Rolph, G.D., Stunder, B.J.B., Cohen, M.D., and Ngan, F., 2015, NOAA's HYSPLIT atmospheric transport and dispersion modeling system: Bulletin of the American Meteorological Society, v. 96, p. 2059–2077, doi: 10.1175/BAMS-D-14-00110.1.

Sun, J., Zhang, Z., and Zhang, L., 2009, New evidence on the age of the Taklimakan Desert: Geology, v. 37, no. 2, p. 159–162, doi: 10.1130/G25338A.1.

Sun, J., Lü, T., Gong, Y., Liu, W., Wang, X., and Gong, Z., 2013, Effect of aridification on carbon isotopic variation and ecologic evolution at 5.3 Ma in the Asian interior: Earth and Planetary Science Letters, v. 380, p. 1–11, doi: 10.1016/j.epsl.2013.08.027.

Tang, Z., Ding, Z., White, P.D., Dong, X., Ji, J., Jiang, H., Luo, P., and Wang, X., 2011, Late Cenozoic central Asian drying inferred from a palynological record from the northern Tian Shan: Earth and Planetary Science Letters, v. 302, no. 3–4, p. 439–447, doi: 10.1016/j.epsl.2010.12.042.

Vangengeim, E.A., Vislobokova, I.A., Godina, A.Y., Dimitrieva, E.L., Zhegallo, V.I., Sotnikova, M.V., and Tleuberdina, P.A., 1993, On the age of mammalian fauna from the Karabulak Formation of the Kalmakpai River (Zaisan Depression, Eastern Kazakhstan): Stratigraphy and Geological Correlation, v. 1, no. 2, p. 165–171.

Winnick, M.J., Chamberlain, C.P., Caves, J.K., and Welker, J.M., 2014, Quantifying the isotopic "continental effect": Earth and Planetary Science Letters, v. 406, p. 123–133, doi: 10.1016/j.epsl.2014.09.005.

Zachos, J., Pagani, M., Sloan, L., Thomas, E., and Billups, K., 2001, Trends, rhythms, and aberrations in global climate 65 Ma to present: Science, v. 292, p. 686–693, doi: 10.1126/science.1059412.

Zhang, Z., Huijun, W., Zhengtang, G., and Dabang, J., 2007, Impacts of tectonic changes on the reorganization of the Cenozoic paleoclimatic patterns in China: Earth and Planetary Science Letters, v. 257, no. 3–4, p. 622–634, doi: 10.1016/j.epsl.2007.03.024.

Zhang, Y., Sun, D., Li, Z., Wang, F., Wang, X., Li, B., Guo, F., and Wu, S., 2014, Cenozoic record of aeolian sediment accumulation and aridification from Lanzhou, China, driven by Tibetan Plateau uplift and global climate: Global and Planetary Change, v. 120, p. 1–15, doi: 10.1016/j.gloplacha.2014.05.009.

Zhisheng, A., Kutzbach, J.E., Prell, W.L., and Porter, S.C., 2001, Evolution of Asian monsoons and phased uplift of the Himalaya-Tibetan plateau since Late Miocene times: Nature, v. 411, 6833, p. 62–66, doi: 10.1038/35075035.

Manuscript received 2 June 2016
Revised manuscript received 5 Sept. 2016
Manuscript accepted 21 Sept. 2016